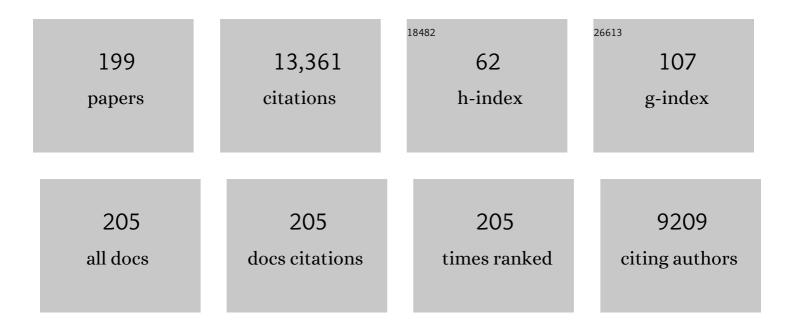
## Yuansheng Wang

List of Publications by Year in descending order

Source: https://exaly.com/author-pdf/6279834/publications.pdf Version: 2024-02-01



#	Article	IF	CITATIONS
1	A new-generation color converter for high-power white LED: transparent Ce <sup>3+</sup> :YAG phosphor-in-glass. Laser and Photonics Reviews, 2014, 8, 158-164.	8.7	519
2	A Novel Optical Thermometry Strategy Based on Diverse Thermal Response from Two Intervalence Charge Transfer States. Advanced Functional Materials, 2016, 26, 3139-3145.	14.9	467
3	CaMg <sub>2</sub> Al <sub>16</sub> O <sub>27</sub> :Mn <sup>4+</sup> -based Red Phosphor: A Potential Color Converter for High-Powered Warm W-LED. ACS Applied Materials & Interfaces, 2014, 6, 22905-22913.	8.0	393
4	Hydrothermal Synthesis, Structural Characteristics, and Enhanced Photocatalysis of SnO <sub>2</sub> /α-Fe <sub>2</sub> O <sub>3</sub> Semiconductor Nanoheterostructures. ACS Nano, 2010, 4, 681-688.	14.6	373
5	Quasicubic α-Fe2O3 Nanoparticles with Excellent Catalytic Performance. Journal of Physical Chemistry B, 2006, 110, 3093-3097.	2.6	332
6	Modifying the Size and Shape of Monodisperse Bifunctional Alkaline-Earth Fluoride Nanocrystals through Lanthanide Doping. Journal of the American Chemical Society, 2010, 132, 9976-9978.	13.7	293
7	Non-Rare-Earth BaMgAl <sub>10–2<i>x</i></sub> O <sub>17</sub> : <i>x</i> Mn <sup>4+</sup> , <i>x</i> Mg <sup>2+</sup> : A Narrow-Band Red Phosphor for Use as a High-Power Warm w-LED. Chemistry of Materials, 2016, 28, 3515-3524.	6.7	290
8	Glass Ceramic Phosphors: Towards Longâ€Lifetime Highâ€Power White Lightâ€Emittingâ€Diode Applications–A Review. Laser and Photonics Reviews, 2018, 12, 1700344.	8.7	256
9	A novel double-perovskite Gd <sub>2</sub> ZnTiO <sub>6</sub> :Mn <sup>4+</sup> red phosphor for UV-based w-LEDs: structure and luminescence properties. Journal of Materials Chemistry C, 2016, 4, 2374-2381.	5.5	240
10	Exploring the Different Photocatalytic Performance for Dye Degradations over Hexagonal Znln <sub>2</sub> S <sub>4</sub> Microspheres and Cubic Znln <sub>2</sub> S <sub>4</sub> Nanoparticles. ACS Applied Materials & Interfaces, 2012, 4, 2273-2279.	8.0	209
11	Tunable Red-Green Upconversion Luminescence in Novel Transparent Glass Ceramics Containing Er:Â NaYF4Nanocrystals. Journal of Physical Chemistry B, 2006, 110, 20843-20846.	2.6	206
12	Bright upconversion white light emission in transparent glass ceramic embedding Tm3+â^•Er3+â^•Yb3+:β-YF3 nanocrystals. Applied Physics Letters, 2007, 91, .	3.3	202
13	Strategy design for ratiometric luminescence thermometry: circumventing the limitation of thermally coupled levels. Journal of Materials Chemistry C, 2018, 6, 7462-7478.	5.5	194
14	Near-infrared quantum cutting in transparent nanostructured glass ceramics. Optics Letters, 2008, 33, 1884.	3.3	184
15	Yb3+/Er3+ co-doped CaMoO4: a promising green upconversion phosphor for optical temperature sensing. Journal of Alloys and Compounds, 2015, 639, 325-329.	5.5	176
16	Phosphor-in-Glass for High-Powered Remote-Type White AC-LED. ACS Applied Materials & Interfaces, 2014, 6, 21264-21269.	8.0	174
17	Lanthanide nanomaterials with photon management characteristics for photovoltaic application. Nano Energy, 2012, 1, 73-90.	16.0	162
18	Quantum cutting downconversion by cooperative energy transfer from Ce3+ to Yb3+ in borate glasses. Journal of Applied Physics, 2008, 104, .	2.5	153

#	Article	IF	CITATIONS
19	Evolution of Single Crystalline Dendrites from Nanoparticles through Oriented Attachment. Journal of Physical Chemistry B, 2005, 109, 794-798.	2.6	152
20	High-security-level multi-dimensional optical storage medium: nanostructured glass embedded with LiGa5O8: Mn2+ with photostimulated luminescence. Light: Science and Applications, 2020, 9, 22.	16.6	152
21	Impurity doping: a novel strategy for controllable synthesis of functional lanthanide nanomaterials. Nanoscale, 2013, 5, 4621.	5.6	146
22	Intense ultraviolet upconversion luminescence from Tm3+â^•Yb3+:β-YF3 nanocrystals embedded glass ceramic. Applied Physics Letters, 2007, 91, .	3.3	145
23	Two-Step Self-Assembly of Nanodisks into Plate-Built Cylinders through Oriented Aggregation. Journal of Physical Chemistry B, 2005, 109, 11548-11551.	2.6	144
24	Bandgap Tailoring via Si Doping in Inverse-Garnet Mg <sub>3</sub> Y <sub>2</sub> Ge <sub>3</sub> O <sub>12</sub> :Ce <sup>3+</sup> Persistent Phosphor Potentially Applicable in AC-LED. ACS Applied Materials & Interfaces, 2015, 7, 21835-21843.	8.0	143
25	Intervalence charge transfer state interfered Pr3+ luminescence: A novel strategy for high sensitive optical thermometry. Sensors and Actuators B: Chemical, 2017, 243, 137-143.	7.8	136
26	Chromaticity-tunable phosphor-in-glass for long-lifetime high-power warm w-LEDs. Journal of Materials Chemistry C, 2015, 3, 8080-8089.	5.5	134
27	Cooperative Energy Transfer Up-Conversion and Quantum Cutting Down-Conversion in Yb <sup>3+</sup> :TbF <sub>3</sub> Nanocrystals Embedded Glass Ceramics. Journal of Physical Chemistry C, 2009, 113, 6406-6410.	3.1	132
28	Metastable γ-MnS Hierarchical Architectures: Synthesis, Characterization, and Growth Mechanism. Journal of Physical Chemistry B, 2006, 110, 8284-8288.	2.6	130
29	Ultra-small yellow defective TiO2 nanoparticles for co-catalyst free photocatalytic hydrogen production. Nano Energy, 2016, 24, 63-71.	16.0	129
30	Ultra-broadband near-infrared excitable upconversion core/shell nanocrystals. Chemical Communications, 2012, 48, 5898.	4.1	125
31	Color-tunable luminescence of Eu3+ in LaF3 embedded nanocomposite for light emitting diode. Acta Materialia, 2010, 58, 3035-3041.	7.9	122
32	Design, Preparation, and Characterization of a Novel Red Long-Persistent Perovskite Phosphor: Ca <sub>3</sub> Ti <sub>2</sub> O <sub>7</sub> :Pr <sup>3+</sup> . Inorganic Chemistry, 2015, 54, 11299-11306.	4.0	122
33	Nonâ€Rareâ€Earth K <sub>2</sub> XF <sub>7</sub> :Mn <sup>4+</sup> (X = Ta, Nb): A Highlyâ€Efficient Narrowâ€Band Red Phosphor Enabling the Application in Wideâ€Colorâ€Gamut LCD. Laser and Photonics Reviews, 2017, 11, 1700148.	8.7	120
34	A highly-distorted octahedron with a C <sub>2v</sub> group symmetry inducing an ultra-intense zero phonon line in Mn <sup>4+</sup> -activated oxyfluoride Na <sub>2</sub> WO <sub>2</sub> F <sub>4</sub> . Journal of Materials Chemistry C, 2017, 5, 10524-10532.	5.5	120
35	Luminescence study of a self-activated and rare earth activated Sr <sub>3</sub> La(VO <sub>4</sub> ) <sub>3</sub> phosphor potentially applicable in W-LEDs. Journal of Materials Chemistry C, 2015, 3, 3023-3028.	5.5	113
36	Dopant-induced phase transition: a new strategy of synthesizing hexagonal upconversion NaYF4 at low temperature. Chemical Communications, 2011, 47, 5801.	4.1	112

#	Article	IF	CITATIONS
37	Synthesis and magnetic properties of nickel ferrite nano-octahedra. Journal of Solid State Chemistry, 2005, 178, 2394-2397.	2.9	106
38	Ultraviolet-blue to near-infrared downconversion of Nd^3+-Yb^3+ couple. Optics Letters, 2010, 35, 220.	3.3	104
39	Phase transition from hexagonal LnF3 (Ln = La, Ce, Pr) to cubic Ln0.8M0.2F2.8 (M = Ca, Sr, Ba) nanocrystals with enhanced upconversion induced by alkaline-earth doping. Chemical Communications, 2011, 47, 2601.	4.1	97
40	Enhanced mid-infrared emissions of Er^3+ at 27 μm via Nd^3+ sensitization in chalcohalide glass. Optics Letters, 2011, 36, 1815.	3.3	97
41	Near-infrared quantum cutting in Ho^3+/Yb^3+ codoped nanostructured glass ceramic. Optics Letters, 2011, 36, 876.	3.3	96
42	Lu <sub>2</sub> CaMg <sub>2</sub> (Si <sub>1â^'x</sub> Ge <sub>x</sub> ) <sub>3</sub> O <sub>12</sub> :Ce <s phosphors: bandgap engineering for blue-light activated afterglow applicable to AC-LED. Journal of Materials Chemistry C, 2016, 4, 10329-10338.</s 	up>3+5.5	up>solid-solı 92
43	Intrinsic single-band upconversion emission in colloidal Yb/Er(Tm):Na3Zr(Hf)F7 nanocrystals. Chemical Communications, 2012, 48, 10630.	4.1	91
44	Highly thermal-stable warm w-LED based on Ce:YAG PiG stacked with a red phosphor layer. Journal of Alloys and Compounds, 2015, 649, 661-665.	5.5	88
45	Lanthanide dopant-induced formation of uniform sub-10 nm active-core/active-shell nanocrystals with near-infrared to near-infrared dual-modal luminescence. Journal of Materials Chemistry, 2012, 22, 2632-2640.	6.7	87
46	Modifying the size and uniformity of upconversion Yb/Er:NaGdF4 nanocrystals through alkaline-earth doping. Nanoscale, 2013, 5, 11298.	5.6	87
47	Broadband UV excitable near-infrared downconversion luminescence in Eu2+/Yb3+:CaF2 nanocrystals embedded glass ceramics. Journal of Alloys and Compounds, 2011, 509, 3363-3366.	5.5	85
48	Shape Control of Monodisperse CdS Nanocrystals:Â Hexagon and Pyramid. Journal of Physical Chemistry B, 2006, 110, 9448-9451.	2.6	81
49	Influences of Er3+ content on structure and upconversion emission of oxyfluoride glass ceramics containing CaF2 nanocrystals. Materials Chemistry and Physics, 2006, 95, 264-269.	4.0	81
50	Structure and Optical Spectroscopy of Eu-Doped Glass Ceramics Containing GdF <sub>3</sub> Nanocrystals. Journal of Physical Chemistry C, 2008, 112, 18943-18947.	3.1	81
51	Color-tunable luminescence for Bi3+/Ln3+:YVO4 (Ln = Eu, Sm, Dy, Ho) nanophosphors excitable by near-ultraviolet light. Physical Chemistry Chemical Physics, 2010, 12, 7775.	2.8	81
52	Structure and luminescence behavior of a single-ion activated single-phased Ba <sub>2</sub> Y <sub>3</sub> (SiO <sub>4</sub> ) <sub>3</sub> F:Eu white-light phosphor. Journal of Materials Chemistry C, 2017, 5, 1789-1797.	5.5	81
53	Lanthanide activator doped NaYb1â~'xGdxF4 nanocrystals with tunable down-, up-conversion luminescence and paramagnetic properties. Journal of Materials Chemistry, 2011, 21, 6186.	6.7	79
54	Broadening the valid temperature range of optical thermometry through dual-mode design. Journal of Materials Chemistry C, 2018, 6, 11178-11183.	5.5	79

#	Article	IF	CITATIONS
55	Novel rare earth ions-doped oxyfluoride nano-composite with efficient upconversion white-light emission. Journal of Solid State Chemistry, 2008, 181, 2763-2767.	2.9	78
56	<scp><scp>Ce</scp></scp> <sup>3+</sup> / <scp><scp>Pr</scp></scp> <sup>3+</sup> : <scp>YAGG</scp> : A Long Persistent Phosphor Activated by Blueâ€Light. Journal of the American Ceramic Society, 2014, 97, 2539-2545.	3.8	78
57	Broadband near-infrared emission from Tm3+â^•Er3+ co-doped nanostructured glass ceramics. Journal of Applied Physics, 2007, 101, 113511.	2.5	71
58	Cr <sup>3+</sup> :SrGa <sub>12</sub> O <sub>19</sub> : A Broadband Nearâ€Infrared Longâ€Persistent Phosphor. Chemistry - an Asian Journal, 2014, 9, 1020-1025.	3.3	71
59	Optical spectroscopy of Eu3+ and Tb3+ doped glass ceramics containing LiYbF4 nanocrystals. Applied Physics Letters, 2009, 94, .	3.3	68
60	Highly Intensified Upconversion Luminescence of Ca <sup>2+</sup> â€doped Yb/Er:NaGdF <sub>4</sub> Nanocrystals Prepared by a Solvothermal Route. Chemistry - an Asian Journal, 2014, 9, 728-733.	3.3	68
61	CsPbBr <sub>3</sub> /EuPO <sub>4</sub> dual-phase devitrified glass for highly sensitive self-calibrating optical thermometry. Journal of Materials Chemistry C, 2018, 6, 9964-9971.	5.5	68
62	CsPb(Br,I)3 embedded glass: Fabrication, tunable luminescence, improved stability and wide-color gamut LCD application. Chemical Engineering Journal, 2019, 378, 122255.	12.7	65
63	Stable CsPbBr <sub>3</sub> â€Glass Nanocomposite for Lowâ€Ã‰tendue Wideâ€Colorâ€Gamut Laserâ€Driven Projection Display. Laser and Photonics Reviews, 2021, 15, 2100044.	8.7	65
64	Inorganic halide perovskite quantum dot modified YAG-based white LEDs with superior performance. Journal of Materials Chemistry C, 2016, 4, 7601-7606.	5.5	64
65	Synthesis and visible light photocatalysis of Fe-doped TiO2 mesoporous layers deposited on hollow glass microbeads. Journal of Solid State Chemistry, 2009, 182, 2785-2790.	2.9	62
66	Energy transfer and up-conversion luminescence in Er3+/Yb3+ co-doped transparent glass ceramic containing YF3 nano-crystals. Ceramics International, 2009, 35, 2619-2623.	4.8	62
67	CeF_3-based glass ceramic: a potential luminescent host for white-light-emitting diode. Optics Letters, 2009, 34, 2882.	3.3	62
68	A novel high-sensitive upconversion thermometry strategy: Utilizing synergistic effect of dual-wavelength lasers excitation to manipulate electron thermal distribution. Sensors and Actuators B: Chemical, 2019, 278, 165-171.	7.8	62
69	Size-dependent abnormal thermo-enhanced luminescence of ytterbium-doped nanoparticles. Nanoscale, 2017, 9, 13794-13799.	5.6	61
70	Spectroscopic properties of Er3+ions in transparent oxyfluoride glass ceramics containing CaF2nano-crystals. Journal of Physics Condensed Matter, 2005, 17, 6545-6557.	1.8	59
71	Tuning of multicolor emissions in glass ceramics containing γ-Ga2O3 and β-YF3 nanocrystals. Journal of Materials Chemistry C, 2013, 1, 1804.	5.5	57
72	MnS Hierarchical Hollow Spheres with Novel Shell Structure. Journal of Physical Chemistry B, 2006, 110, 24399-24402.	2.6	56

#	Article	IF	CITATIONS
73	Sn2+/Mn2+ codoped strontium phosphate (Sr2P2O7) phosphor for high temperature optical thermometry. Journal of Alloys and Compounds, 2018, 735, 1546-1552.	5.5	56
74	Microstructure and luminescence of transparent glass ceramic containing Er3+:BaF2 nano-crystals. Journal of Solid State Chemistry, 2006, 179, 532-537.	2.9	55
75	Partition, luminescence and energy transfer of Er3+/Yb3+ ions in oxyfluoride glass ceramic containing CaF2 nano-crystals. Optical Materials, 2007, 29, 1693-1699.	3.6	55
76	A Photostimulated BaSi <sub>2</sub> O <sub>5</sub> :Eu <sup>2+</sup> ,Nd <sup>3+</sup> Phosphorâ€inâ€Glass for Erasableâ€Rewritable Optical Storage Medium. Laser and Photonics Reviews, 2019, 13, 1900006.	8.7	55
77	X-ray excited CsPb(Cl,Br)3 perovskite quantum dots-glass composite with long-lifetime. Journal of the European Ceramic Society, 2020, 40, 2234-2238.	5.7	55
78	Enhanced emissions of Eu <sup>3+</sup> by energy transfer from ZnO quantum dots embedded in SiO <sub>2</sub> glass. Nanotechnology, 2008, 19, 055711.	2.6	54
79	pH value-dependant growth of α-Fe2O3 hierarchical nanostructures. Journal of Crystal Growth, 2006, 294, 353-357.	1.5	53
80	CuGaS <sub>2</sub> –ZnS p–n nanoheterostructures: a promising visible light photo-catalyst for water-splitting hydrogen production. Nanoscale, 2016, 8, 16670-16676.	5.6	52
81	Color-tunable persistent luminescence in oxyfluoride glass and glass ceramic containing Mn <sup>2+</sup> :α-Zn <sub>2</sub> SiO <sub>4</sub> nanocrystals. Journal of Materials Chemistry C, 2017, 5, 1479-1487.	5.5	52
82	Monodisperse upconversion Er3+/Yb3+:MFCl (M = Ca, Sr, Ba) nanocrystals synthesized via a seed-based chlorination route. Chemical Communications, 2011, 47, 11083.	4.1	51
83	Stress-induced CsPbBr3 nanocrystallization on glass surface: Unexpected mechanoluminescence and applications. Nano Research, 2019, 12, 1049-1054.	10.4	50
84	Influence of Yb3+ content on microstructure and fluorescence of oxyfluoride glass ceramics containing LaF3 nano-crystals. Materials Chemistry and Physics, 2007, 101, 464-469.	4.0	49
85	Nanocrystallization of lanthanide trifluoride in an aluminosilicate glass matrix: dimorphism and rare earth partition. CrystEngComm, 2009, 11, 1686.	2.6	49
86	A chromaticity-tunable garnet-based phosphor-in-glass color converter applicable in w-LED. Journal of the European Ceramic Society, 2016, 36, 1723-1729.	5.7	49
87	Fluorescence and Judd–Ofelt analysis of Nd3+ ions in oxyfluoride glass ceramics containing CaF2 nanocrystals. Journal of Physics and Chemistry of Solids, 2007, 68, 193-200.	4.0	48
88	Transparent glass ceramic containing Er3+:CaF2 nano-crystals prepared by sol–gel method. Materials Letters, 2007, 61, 3988-3990.	2.6	48
89	Upconversion luminescence of Ho3+ sensitized by Yb3+ in transparent glass ceramic embedding BaYF5 nanocrystals. Materials Research Bulletin, 2010, 45, 1017-1020.	5.2	48
90	A new transparent oxyfluoride glass ceramic with improved luminescence. Journal of Non-Crystalline Solids, 2007, 353, 405-409.	3.1	46

#	Article	IF	CITATIONS
91	Sensitized thulium ultraviolet upconversion luminescence in Tm^3+/Yb^3+/Nd^3+ triply doped nanoglass ceramics. Optics Letters, 2007, 32, 3068.	3.3	45
92	Judd–Ofelt analyses and luminescence of Er3+/Yb3+ co-doped transparent glass ceramics containing NaYF4 nanocrystals. Journal of Alloys and Compounds, 2010, 490, 74-77.	5.5	45
93	An active-core/active-shell structure with enhanced quantum-cutting luminescence in Pr–Yb co-doped monodisperse nanoparticles. Nanoscale, 2014, 6, 10500-10504.	5.6	45
94	Enhancing negative thermal quenching effect <i>via</i> low-valence doping in two-dimensional confined core–shell upconversion nanocrystals. Journal of Materials Chemistry C, 2018, 6, 11587-11592.	5.5	45
95	Hydrothermal synthesis and characterization of MnWO4 nanoplates and their ionic conductivity. Materials Chemistry and Physics, 2007, 103, 433-436.	4.0	44
96	Molecular-like Ag clusters sensitized near-infrared down-conversion luminescence in oxyfluoride glasses for broadband spectral modification. Applied Physics Letters, 2013, 103, .	3.3	44
97	Plasmon-driven N <sub>2</sub> photofixation in pure water over MoO <sub>3â^x</sub> nanosheets under visible to NIR excitation. Journal of Materials Chemistry A, 2020, 8, 2827-2835.	10.3	44
98	Upconversion emission of a novel glass ceramic containing Er3+: BaYF5 nano-crystals. Materials Letters, 2007, 61, 5022-5025.	2.6	43
99	Infrared luminescence of transparent glass ceramic containing Er3+:NaYF4 nanocrystals. Journal of Alloys and Compounds, 2009, 467, 317-321.	5.5	43
100	Luminescence in rare earth-doped transparent glass ceramics containing GdF3 nanocrystals for lighting applications. Journal of Materials Science, 2010, 45, 2775-2779.	3.7	43
101	A visible light active photocatalyst: Nano-composite with Fe-doped anatase TiO2 nanoparticles coupling with TiO2(B) nanobelts. Journal of Molecular Catalysis A, 2010, 326, 1-7.	4.8	43
102	Host-sensitized multicolor tunable luminescence of lanthanide ion doped one-dimensional YVO4 nano-crystals. Journal of Alloys and Compounds, 2011, 509, 3375-3381.	5.5	43
103	Synergistic effect of the rearranged sulfur vacancies and sulfur interstitials for 13-fold enhanced photocatalytic H2 production over defective Zn2In2S5 nanosheets. Applied Catalysis B: Environmental, 2019, 240, 270-276.	20.2	43
104	Crystallization behavior and microstructure investigations on LaF3 containing oxyfluoride glass ceramics. Journal of Non-Crystalline Solids, 2005, 351, 722-728.	3.1	42
105	Nd3+-sensitized upconversion white light emission of Tm3+/Ho3+ bridged by Yb3+ in β-YF3 nanocrystals embedded transparent glass ceramics. Journal of Applied Physics, 2010, 107, 103511.	2.5	42
106	Crystallization and fluorescence properties of Nd3+-doped transparent oxyfluoride glass ceramics. Materials Science and Engineering B: Solid-State Materials for Advanced Technology, 2005, 123, 1-6.	3.5	41
107	Abnormal thermally enhanced upconversion luminescence of lanthanide-doped phosphors: proposed mechanisms and potential applications. Journal of Materials Chemistry C, 2021, 9, 2220-2230.	5.5	41
108	Towards long-lifetime high-performance warm w-LEDs: Fabricating chromaticity-tunable glass ceramic using an ultra-low melting Sn-P-F-O glass. Journal of the European Ceramic Society, 2018, 38, 1990-1997.	5.7	40

#	Article	IF	CITATIONS
109	Patterned glass ceramic design for high-brightness high-color-quality laser-driven lightings. Journal of Advanced Ceramics, 2022, 11, 862-873.	17.4	40
110	Narrow-band red-emitting KZnF <sub>3</sub> :Mn <sup>4+</sup> fluoroperovskites: insights into electronic/vibronic transition and thermal quenching behavior. Journal of Materials Chemistry C, 2018, 6, 10845-10854.	5.5	39
111	Abnormal size-dependent upconversion emissions and multi-color tuning in Er <sup>3+</sup> -doped CaF <sub>2</sub> –YbF <sub>3</sub> disordered solid-solution nanocrystals. Nanotechnology, 2013, 24, 085708.	2.6	38
112	Heating-induced abnormal increase in Yb <sup>3+</sup> excited state lifetime and its potential application in lifetime luminescence nanothermometry. Inorganic Chemistry Frontiers, 2019, 6, 110-116.	6.0	38
113	βâ€SiAlON:Eu <sup>2+</sup> Phosphorâ€inâ€Glass Film: An Efficient Laserâ€Driven Color Converter for Highâ€Brightness Wideâ€Colorâ€Gamut Projection Displays. Laser and Photonics Reviews, 2021, 15, 2100317.	8.7	37
114	Toward Highâ€Quality Laserâ€Driven Lightings: Chromaticityâ€Tunable Phosphorâ€inâ€Glass Film with "Phosphor Pattern―Design. Laser and Photonics Reviews, 2022, 16, .	8.7	37
115	Dual-mode color tuning based on upconversion core/triple-shell nanostructure. Journal of Materials Chemistry C, 2019, 7, 3342-3350.	5.5	35
116	Improvement of Er3+ emissions in oxyfluoride glass ceramic nano-composite by thermal treatment. Journal of Solid State Chemistry, 2006, 179, 1445-1452.	2.9	34
117	Microstructures and upconversion luminescence of Er3+ doped and Er3+/Yb3+ co-doped oxyfluoride glass ceramics. Materials Chemistry and Physics, 2007, 101, 234-237.	4.0	34
118	Enhanced luminescence in Ce3+/Dy3+: Sr3Y2(BO3)4 phosphors via energy transfer. Materials Research Bulletin, 2013, 48, 1957-1960.	5.2	34
119	Formation of AgGaS2 nano-pyramids from Ag2S nanospheres through intermediate Ag2S–AgGaS2 heterostructures and AgGaS2 sensitized Mn2+ emission. Nanoscale, 2014, 6, 2340.	5.6	33
120	Towards ultra-high sensitive colorimetric nanothermometry: Constructing thermal coupling channel for electronically independent levels. Sensors and Actuators B: Chemical, 2018, 256, 498-503.	7.8	33
121	SnO2/α-Fe2O3 nanoheterostructure with novel architecture: structural characteristics and photocatalytic properties. CrystEngComm, 2011, 13, 4873.	2.6	32
122	Synthesis and shape evolution of α-Fe2O3 nanophase through two-step oriented aggregation in solvothermal system. Journal of Crystal Growth, 2005, 284, 221-225.	1.5	31
123	Multiple branched α-MnO2 nanofibers: A two-step epitaxial growth. Journal of Crystal Growth, 2006, 286, 156-161.	1.5	30
124	Novel Nanocrystal Heterostructures: Crystallographic-Oriented Growth of SnO <sub>2</sub> Nanorods onto α-Fe <sub>2</sub> O <sub>3</sub> Nanohexahedron. Crystal Growth and Design, 2008, 8, 1727-1729.	3.0	30
125	Thermo-enhanced upconversion luminescence in inert-core/active-shell UCNPs: the inert core matters. Nanoscale, 2021, 13, 6569-6576.	5.6	30
126	Design of Ratiometric Dualâ€Emitting Mechanoluminescence: Lanthanide/Transitionâ€Metal Combination Strategy. Laser and Photonics Reviews, 2022, 16, .	8.7	30

#	Article	IF	CITATIONS
127	Investigation on crystallization kinetics and microstructure of novel transparent glass ceramics containing Nd:NaYF4 nano-crystals. Materials Science and Engineering B: Solid-State Materials for Advanced Technology, 2007, 136, 106-110.	3.5	29
128	Highly efficient nearâ€infrared to visible upconversion luminescence in transparent glass ceramics containing Yb <sup>3+</sup> /Er <sup>3+</sup> :NaYF <sub>4</sub> nanocrystals. Physica Status Solidi (A) Applications and Materials Science, 2008, 205, 1680-1684.	1.8	28
129	Integrated broadband near-infrared luminescence in transparent glass ceramics containing γ-Ga2O3: Ni2+ and β-YF3: Er3+ nanocrystals. Journal of Alloys and Compounds, 2013, 552, 398-404.	5.5	28
130	Influence of structural evolution on fluorescence properties of transparent glass ceramics containing LaF3 nanocrystals. Journal of Luminescence, 2006, 118, 131-138.	3.1	27
131	Enhanced photoluminescence of Eu3+ induced by energy transfer from In2O3 nano-crystals embedded in glassy matrix. Physical Chemistry Chemical Physics, 2009, 11, 8774.	2.8	27
132	Structure and luminescence of Eu3+ doped glass ceramics embedding ZnO quantum dots. Ceramics International, 2010, 36, 1091-1094.	4.8	27
133	Crystallization and spectroscopic properties investigations of Er3+ doped transparent glass ceramics containing CaF2. Materials Research Bulletin, 2006, 41, 217-224.	5.2	26
134	Investigation on crystallization and influence of Nd3+ doping of transparent oxyfluoride glass-ceramics. Journal of the European Ceramic Society, 2006, 26, 2761-2767.	5.7	25
135	A blue-emitting Sc silicate phosphor for ultraviolet excited light-emitting diodes. Physical Chemistry Chemical Physics, 2015, 17, 27292-27299.	2.8	25
136	Host sensitization of Mn <sup>4+</sup> in selfâ€activated Na <sub>2</sub> WO <sub>2</sub> F <sub>4</sub> :Mn <sup>4+</sup> . Journal of the American Ceramic Society, 2018, 101, 3437-3442.	3.8	23
137	Crystallization and structural evolution of YF3–SiO2 xerogel. Materials Science and Engineering B: Solid-State Materials for Advanced Technology, 2006, 127, 218-223.	3.5	22
138	Controllable synthesis of metal selenide heterostructures mediated by Ag2Se nanocrystals acting as catalysts. Nanoscale, 2013, 5, 9714.	5.6	22
139	Perceiving Linear-Velocity by Multiphoton Upconversion. ACS Applied Materials & Interfaces, 2019, 11, 46379-46385.	8.0	22
140	A solid-state colorimetric fluorescence Pb <sup>2+</sup> -sensing scheme: mechanically-driven CsPbBr <sub>3</sub> nanocrystallization in glass. Nanoscale, 2020, 12, 8801-8808.	5.6	22
141	Crystallization behavior of PbF2–SiO2 based bulk xerogels. Journal of Non-Crystalline Solids, 2004, 347, 31-38.	3.1	21
142	Cu1.94S–MnS dimeric nanoheterostructures with bifunctions: localized surface plasmon resonance and magnetism. CrystEngComm, 2013, 15, 4217.	2.6	21
143	Phase transition and multicolor luminescence of Eu2+/Mn2+-activated Ca3(PO4)2 phosphors. Materials Research Bulletin, 2014, 49, 677-681.	5.2	21
144	Doped polyaniline-hybridized tungsten oxide nanocrystals as hole injection layers for efficient organic light-emitting diodes. Journal of Materials Chemistry C, 2018, 6, 7242-7248.	5.5	21

#	Article	IF	CITATIONS
145	Luminescence of an Er3+-doped glass matrix containing CdS quantum dots. Scripta Materialia, 2006, 55, 891-894.	5.2	20
146	A plasmonic nano-antenna with controllable resonance frequency: Cu1.94S–ZnS dimeric nanoheterostructure synthesized in solution. Journal of Materials Chemistry, 2012, 22, 22614.	6.7	20
147	Spectroscopic and stimulated emission characteristics of Nd3+ in transparent glass ceramic embedding l²-YF3 nanocrystals. Journal of Applied Physics, 2007, 102, .	2.5	19
148	Spectroscopic calculation of NaYF4 contained transparent glass ceramics doped with different content of Nd3+. Journal of Alloys and Compounds, 2007, 443, 143-148.	5.5	19
149	Spectroscopic properties of Nd3+ doped transparent oxyfluoride glass ceramics. Spectrochimica Acta - Part A: Molecular and Biomolecular Spectroscopy, 2007, 67, 709-713.	3.9	19
150	Syntheses and optical properties of monodisperse BaLnF5 (Ln=La–Lu, Y) nanocrystals. Journal of Alloys and Compounds, 2012, 540, 27-31.	5.5	19
151	Infrared to ultraviolet upconversion luminescence in Nd3+ doped nano-glass-ceramic. Journal of Rare Earths, 2008, 26, 428-432.	4.8	18
152	Distribution-related luminescence of Eu3+ sensitized by SnO2 nano-crystals embedding in oxide glassy matrix. Journal of Solid State Chemistry, 2011, 184, 236-240.	2.9	18
153	Uniform Eu3+:CeO2 hollow microspheres formation mechanism and optical performance. Journal of Alloys and Compounds, 2012, 534, 64-69.	5.5	18
154	Efficient upconversion luminescence of Er3+:SrF2–SiO2–Al2O3 sol–gel glass ceramics. Ceramics International, 2008, 34, 2143-2146.	4.8	17
155	Facile Synthesis and Formation Mechanism of Metal Chalcogenides Hollow Nanoparticles. Journal of Physical Chemistry C, 2009, 113, 7522-7525.	3.1	17
156	Influence of Er3+ doping on microstructure of oxyfluoride glass–ceramics. Materials Research Bulletin, 2005, 40, 1645-1653.	5.2	16
157	Fluorescence property investigations on Er3+-doped oxyfluoride glass ceramics containing LaF3 nanocrystals. Materials Chemistry and Physics, 2006, 100, 308-312.	4.0	16
158	Color-filtered phosphor-in-glass for LED-lit LCD with wide color gamut. Ceramics International, 2019, 45, 14432-14438.	4.8	16
159	Phase separation in yttrium silicate glass prepared by the sol–gel method. Journal of Non-Crystalline Solids, 2005, 351, 3114-3120.	3.1	15
160	Eu2+:SrMg1â^'xMnxP2O7 (x=0–1) phosphors with tunable yellow–red emissions. Journal of Alloys and Compounds, 2013, 555, 45-50.	5.5	15
161	Nanostructured NdF3 glass ceramic: An efficient bandpass color filter for wide-color-gamut white LED. Journal of the European Ceramic Society, 2019, 39, 2155-2160.	5.7	15
162	Structural evolution and its influence on luminescence of SiO2–SrF2–ErF3 glass ceramics prepared by sol–gel method. Materials Chemistry and Physics, 2006, 100, 241-245.	4.0	14

#	Article	IF	CITATIONS
163	Fabrication of Co3O4 cubic nanoframes: Facet-preferential chemical etching of Fe3+ ions to Co3O4 nanocubes. Materials Letters, 2009, 63, 837-839.	2.6	14
164	High-content bulk doping and thermal stability of rare earth ions in CeO2 nanocrystals. Scripta Materialia, 2010, 63, 661-664.	5.2	14
165	Modifying the phase and controlling the size of monodisperse ZrO2 nanocrystals by employing Gd3+ as a nucleation agent. CrystEngComm, 2011, 13, 4500.	2.6	14
166	Ultraviolet upconversion luminescence of Gd3+ and Eu3+ in nano-structured glass ceramics. Materials Research Bulletin, 2012, 47, 469-472.	5.2	14
167	Toward high-power-density laser-driven lighting: enhancing heat dissipation in phosphor-in-glass film by introducing h-BN. Optics Letters, 2022, 47, 3455.	3.3	14
168	Improving Er3+ 1.53â€,μm luminescence by CeF3 nanocrystallization in aluminosilicate glass. Journal of Applied Physics, 2010, 108, 123523.	2.5	13
169	Tm3+-sensitized up- and down-conversions in nano-structured oxyfluoride glass ceramics. Materials Research Bulletin, 2012, 47, 4433-4437.	5.2	13
170	Impact of High Ytterbium(III) Concentration in the Shell on Upconversion Luminescence of Core–Shell Nanocrystals. Chemistry - an Asian Journal, 2014, 9, 2765-2770.	3.3	13
171	Luminescence at 1.53μm for a new Er3+-doped transparent oxyfluoride glass ceramic. Materials Research Bulletin, 2006, 41, 1112-1117.	5.2	12
172	Optical spectroscopy investigation on distribution of Eu3+ in nanostructured glass ceramics. Journal of Applied Physics, 2010, 107, 093504.	2.5	12
173	Sensitization and protection of Eu3+ luminescence by CeO2 in nano-composite. Journal of Alloys and Compounds, 2012, 513, 626-629.	5.5	12
174	Sandwich-like Cu <sub>1.94</sub> S–ZnS–Cu <sub>1.94</sub> S nanoheterostructure: structure, formation mechanism and localized surface plasmon resonance behavior. Nanotechnology, 2012, 23, 425604.	2.6	12
175	The synergistic role of double vacancies within AgGaS <sub>2</sub> nanocrystals in carrier separation and transfer for efficient photocatalytic hydrogen evolution. Catalysis Science and Technology, 2019, 9, 5838-5844.	4.1	12
176	Boosting single-band red upconversion luminescence in colloidal NaErF4 nanocrystals: Effects of doping and inert shell. Journal of Rare Earths, 2019, 37, 573-579.	4.8	11
177	Fabrication and structure characterization of MnCO3/α-Fe2O3 nanocrystal heterostructures. Materials Letters, 2009, 63, 2499-2502.	2.6	10
178	Co <sup>2+</sup> /Er <sup>3+</sup> co-doped transparent glass ceramic containing both spinel ZnAl <sub>2</sub> O <sub>4</sub> and orthorhombic YF <sub>3</sub> for self- <i>Q</i> -switched laser. Laser Physics, 2014, 24, 025101.	1.2	10
179	Utilizing Au–CuS heterodimer to intensify upconversion emission of NaGdF4:Yb/Er nanocrystals. Journal of Materials Science, 2020, 55, 6891-6902.	3.7	10
180	Pumping-controlled multicolor modulation of upconversion emission for dual-mode dynamic anti-counterfeiting. Nanophotonics, 2020, 9, 1519-1528.	6.0	10

#	Article	IF	CITATIONS
181	In-situ creating elastic lattice O O bonds over semicrystalline yellow TiO2 nanoparticles for significantly enhanced photocatalytic H2 production. Journal of Hazardous Materials, 2019, 374, 287-295.	12.4	9
182	Self-assembly of mono-crystalline NdF3 nanostructures during hydrothermal process. Materials Letters, 2006, 60, 389-392.	2.6	8
183	Crystallization behaviours of In2.67S4 nanophase in chalcohalide glasses. CrystEngComm, 2011, 13, 3008.	2.6	8
184	Crystallization mechanism and optical properties of Nd3+ doped chalcohalide glass ceramics. Materials Research Bulletin, 2012, 47, 3078-3082.	5.2	8
185	Concentration quenching in transparent glass ceramics containing Er3+:NaYF4 nanocrystals. Science China: Physics, Mechanics and Astronomy, 2012, 55, 1148-1151.	5.1	8
186	Solution Growth of Modified Ultrathin W <sub>18</sub> O <sub>49</sub> Nanobelts with Enhanced Chemical Activity against Alkylamine Radicals. Chemistry - an Asian Journal, 2017, 12, 524-529.	3.3	8
187	Selective-controlled synthesis of one-dimensional strontium phosphates. Journal of Crystal Growth, 2005, 280, 569-574.	1.5	7
188	Synthesis and upconversion emission of rare earth-doped olive-like YF3 micro-particles. Materials Research Bulletin, 2010, 45, 52-55.	5.2	7
189	Reversible self-assembly of MxS (M = Cu, Ag) nanocrystals through ligand exchange. CrystEngComm, 2014, 16, 9478-9481.	2.6	7
190	Growth of hexagonal NaGdF4 nanocrystals based on cubic Ln3+: CaF2 precursors and the multi-color upconversion emissions. Journal of Alloys and Compounds, 2014, 591, 370-376.	5.5	7
191	Laser-direct-writing of molecule-like Ag <sub><i>m</i></sub> <sup><i>x</i>+</sup> nanoclusters in transparent tellurite glass for 3D volumetric optical storage. Nanoscale, 2021, 13, 19663-19670.	5.6	7
192	Converting Ag <sub>2</sub> Sï£;CdS and Ag <sub>2</sub> Sï£;ZnS into Agï£;CdS and Agï£;ZnS Nanoheterostructures by Selective Extraction of Sulfur. Chemistry - an Asian Journal, 2014, 9, 3287-3290.	3.3	6
193	Phase-separation induced homogeneous nucleation and growth of Cs3LaCl6 nanoparticles in chalcohalide glass. Materials Research Bulletin, 2014, 49, 193-198.	5.2	5
194	Simulation of clusters formation in Al-Cu based and Al-Zn based alloys. Journal of Materials Science, 2005, 40, 3461-3466.	3.7	3
195	Advances in spectral conversion for photovoltaics: up-converting Er <sup>3+</sup> doped YF 3 nano-crystals in transparent glass ceramic. Proceedings of SPIE, 2011, , .	0.8	3
196	Broadband excitation of upconversion in lanthanide doped fluorides for enhancement of Si solar cells. , 2012, , .		2
197	Controllable synthesis and selective doping of hexagonal GdF3 and spinel-like Ga2O3 nano-crystals in silicate glass. Ceramics International, 2015, 41, 14197-14203.	4.8	2
198	Inflection in size-dependence of thermally enhanced up-conversion luminescence of UCNPs. Inorganic Chemistry Frontiers, 0, , .	6.0	1

#	Article	IF	CITATIONS
199	All-inorganic Y3Al5O12:Ce3+, Mn2+ Phosphor-in-Glass for Warm W-LED. , 2019, , .		0